POLITECNICO DI TORINO
Repository ISTITUZIONALE

Layer-Wise modeling of temperature distributions and degree of cure to evaluate process-induced deformation and residual stress

Original
Layer-Wise modeling of temperature distributions and degree of cure to evaluate process-induced deformation and residual stress / Zappino, E., Petrolo, M., Santori, M.. - ELETTRONICO. - (2024). (ASME 2024 Aerospace Structures, Structural Dynamics, and Materials Conference SSDM2024 April 29 - May 1, 2024, Renton, Washington Renton, WA, USA 29 April - 1 May 2024).

Availability:
This version is available at: 11583/2988225 since: 2024-05-01T12:45:50Z

Publisher:
ASME

Published
DOI:

Terms of use:

This article is made available under terms and conditions as specified in the corresponding bibliographic description in the repository

Publisher copyright
ASME postprint/Author's accepted manuscript

(Article begins on next page)

15 October 2026

Proceedings of the ASME 2024
Aerospace Structures, Structural Dynamics, and Materials Conference
SSDM2024
April 29 - May 1, 2024, Renton, Washington

SSDM2024-121553

Attendee Read-Only Copy

LAYER-WISE MODELING OF TEMPERATURE DISTRIBUTIONS AND DEGREE OF CURE TO EVALUATE PROCESS-INDUCED DEFORMATION AND RESIDUAL STRESS

Enrico Zappino[1], Marco Petrolo[1], Martina Santori[1]

[1]MUL2 Lab, Department of Mechanical and Aerospace Engineering, Politecnico di Torino, 10129 Turin, Italy

ABSTRACT

In this work, a cure simulation based on a one-dimensional thermochemical model is used to predict the evolution of temperature and degree of cure along the thickness of the composite component during the curing cycle. The one-dimensional heat transfer governing equation through the thickness is coupled with the curing kinetics of the thermoset composite material. Temperatures and degree of cure are then used for a thermo-mechanical analysis using layer-wise 1D elements based on the Carrera Unified Formulation (CUF).
Using 1D models allows for computational costs and enables fast numerical analyses. The impact that thickness has on process-induced stresses and strains is evaluated. In particular, displacements for two flat plates with different layer thicknesses at the end of the process are calculated, and in-plane stress distributions are considered.
The results show the influence of a non-uniform degree of cure along the thickness, resulting in a consequent variation of material properties depending on the layer considered.

Keywords: Cure simulation; Carrera Unified Formulation; Process-induced deformation; Residual stress

NOMENCLATURE

α	Degree of cure, [-]
T	Temperature, [°C]
σ	Stress vector, [Pa]
ε	Strain vector, [-]
E	Young modulus, [Pa]
G	Shear modulus, [Pa]
β	Thermal expansion coefficient, [1/°C]

1. INTRODUCTION

Composite materials have increasingly caught on in the aerospace and automotive industries due to their excellent mechanical properties [1]. The use of an autoclave in the curing process of composite materials allows for increased mechanical performance, but at the same time, it can lead to residual stresses and strains [2]. The change in volume of the composite part is due to both the heating to which it is subjected during the process and the exothermic chemical reactions that occur during polymerization and generate chemical resin shrinkage. Other factors contributing to the dimensional change are shape, orthotropic properties of the part, and the tool-part interaction [3-5]. During the process, the thermal expansion mismatch of fiber and matrix, chemical shrinkage, and the change of state of the resin from fluid to solid lead to the formation of residual stresses [6]. These induced stresses are partially released when the tool is removed, generating a spring-in angle and warpage [7]. The formation of process-induced defects can create assembly problems and reduce the fatigue life of the part [8,9] and is particularly critical in the production of composite aerospace structures due to strict requirements concerning geometric tolerances. Many experimental studies have investigated the effect of process parameters on induced deformations and stresses [10-12]. Experimental tests require high costs, material waste, and time-intensive procedures. The development of models for numerical simulations is, then, desirable to quickly and accurately predict the final shape of the part and design countermeasures.

Predicting temperature distribution and degree of cure distributions during the process is the first step in assessing residual strains and stresses. Software like RAVEN facilitates the simulation of the curing process and the evolution of mechanical properties in composites. Numerical simulations, mainly based on a 1D thermochemical model [13], help predict temperature and degree of cure throughout the thickness of the part. The composite's elastic material properties, chemical shrinkage, and thermal expansion coefficients are evaluated based on the fiber and matrix properties.

The widely utilized Cure Hardening Instantaneously Linear Elastic (CHILE) [14-15] approach involves calculating material properties as averages at each time step and summing these

Copyright © 2024 by ASME

values to derive end-of-process solutions. This methodology is implemented in commercial FE software like COMPRO.

Numerical models based on the finite element method are usually used to evaluate deformations and induced stresses [16-18]. These models are often very sophisticated and thus require high computational costs. In the present work, a refined one-dimensional model [19], based on Carrera Unified Formulation (CUF) [20], is used to predict process-induced deformations accurately and stresses with low computational costs. In particular, composite materials are often used in aerospace, characterised by slender structures. This underlines the preference for 1D models, which provide an optimal balance between accuracy and computational efficiency in such applications. Process analysis is carried out using the CHILE approach. A one-dimensional thermochemical model is used to evaluate trends of degree of cure and temperature in composites. On the other hand, material elastic properties, chemical shrinkage, and thermal expansion coefficients are obtained through a micromechanical model based on the law of mixtures [13].

2. THERMOCHEMICAL MODEL

The 1D thermochemical model, used to find the temperature and degree of cure over the thickness during the cure cycle, consists of two coupled equations. The first equation provides the one-dimensional Fourier heat conduction through thickness:

$$\dot{Q} + k\,\frac{\partial^2 T}{\partial z^2} = \rho c_p \frac{\partial T}{\partial t} \quad \text{for } T(z,t) \text{ in } (0 < z < l) \tag{1}$$

where k is the thermal conductivity, ρ is the density of the composite, l is the thickness, and c_p is the specific heat. The temperature T varies along the z direction normal to the median plane and along time t. The internally generated heat $\dot{Q}$ stems from the exothermic chemical reaction of the resin and it is equal to:

$$\dot{Q} = \rho H_r V_r \frac{d\alpha}{dt} \tag{2}$$

where H_r is the total heat released from the resin reaction, V_r is the volume fraction of the resin, and α is the degree of cure.

The second equation describes the cure kinetics and was proposed by Johnston and Hubert [17,18] for a carbon fiber-reinforced Hexcel 8552 resin:

$$\frac{d\alpha}{dt} = \frac{K\alpha^m (1-\alpha^n)}{1+e^{C[\alpha-(\alpha_{C0}+\alpha_{CT}T)]}} \tag{3}$$

The parameter K is defined by the Arrhenius equation:

$$K = A\, e^{\frac{\Delta E}{RT}} \tag{4}$$

The parameters m, n, C, A, α_{C0} and α_{CT} are obtained experimentally, ΔE is the activation energy, and R is the universal gas constant. The values of these parameters are given in Table 1.

TABLE 1: NUMERICAL VALUES OF THE PARAMETERS IN THE CURE KINETIC EQUATION.

AS4/8852	
m	0.8129
n	2.736
A	$1.528 \cdot 10^5$
$\Delta E\ [J/mol]$	$6.65 \cdot 10^4$
α_{C0}	-1.684
α_{CT}	$5.475 \cdot 10^{-3}$
$H_r\ [kJ/kg]$	550

2.1 Boundary conditions

Generalized boundary conditions can be expressed through the following relationship [13]:

$$a\frac{\partial T_s}{\partial z} + bT_s + cT(t) = 0 \quad for\ x = 0\ and\ x = L \tag{5}$$

where T_s is the surface temperature and T is the temperature of the autoclave. The values of coefficients a, b, and c depend on the type of condition applied to the top and bottom surfaces of the part and are given in Table 2.

TABLE 2: GENERALISED BOUNDARY CONDITION COEFFICIENTS.

Condition	a	b	c
Dirichlet	0	1	-1
Neumann	1	0	0
Robin	1	$(h/k)_{eff}$	$-(h/k)_{eff}$

Dirichlet's boundary conditions impose a part surface temperature equal to room temperature. By setting the Neumann condition instead, the surface has a prescribed temperature. The convection condition corresponds to Robin's condition. The parameter $(h/k)_{eff}$ is the effective heat transfer coefficient divided by the effective thermal conductivity. In this work, on the top surface, convection is applied; on the bottom surface, on the other hand, the presence of the tool is simulated through the Dirichlet condition. The tool's material has high thermal conduction, i.e., the temperature on the bottom surface can be set equal to the temperature of the autoclave.

2.2 Finite element formulation

A finite element formulation was derived to solve the system of equations of the thermochemical model [21]. The 1D model of the part is divided into a number of elements. Denoting the shape functions by $\boldsymbol{N}$, the approximate solution of the temperature $T^e(z,t)$ in each element is obtained through the nodal temperatures:

Copyright © 2024 by ASME

$$T^e(z,t) = \boldsymbol{N}(z)\boldsymbol{T}^e(t) \quad (6)$$

with:

$$\boldsymbol{N}(z) = [N_1(z), N_2(z), \dots, N_m(z)] \quad (7)$$
$$\boldsymbol{T}^e(t) = [T_1^e(t), T_2^e(t), \dots, T_m^e(t)] \quad (8)$$

where $\boldsymbol{T}^e$ is the vector of nodal temperatures and m is the number of nodes in the element. The derivative with respect to z of the temperature is expressed as:

$$\frac{\partial T^e}{\partial z} = \frac{\partial \boldsymbol{N}}{\partial z}\boldsymbol{T}^e = \boldsymbol{B}(z)\boldsymbol{T}^e(t) \quad (9)$$

where $\boldsymbol{B}$ contains derivative of the shape functions. The internally generated heat $\dot{Q}$ can also be expressed by applying the finite element approximation:

$$\dot{Q}(z,t) = \boldsymbol{N}(z)\boldsymbol{b}^e(t) \quad (10)$$

with:

$$\boldsymbol{b}(t) = [\dot{Q}_1(t), \dot{Q}_2(t), \dots, \dot{Q}_n(t)] \quad (11)$$

The heat transfer equation written according to the finite element formulation can be derived using Galerkin's method. The terms of the equation are integrated into the domain of the single element, $[z_i, z_j]$:

$$\boldsymbol{C}^e\dot{\boldsymbol{T}}^e + \boldsymbol{K}^e\boldsymbol{T}^e = \boldsymbol{q}^e + \boldsymbol{M}^e\boldsymbol{b}^e \quad (12)$$

with:

$$\boldsymbol{C}^e = \int_{z_i}^{z_j} \boldsymbol{N}^T\boldsymbol{N}dz \quad (13)$$
$$\boldsymbol{K}^e = \frac{k_c}{\rho c_p}\int_{z_i}^{z_j} \boldsymbol{N}^T\boldsymbol{B}dz \quad (14)$$
$$\boldsymbol{q}^e = \frac{k_c}{\rho c_p}[\boldsymbol{N}^T\boldsymbol{B}\boldsymbol{T}^e]_{z_i}^{z_j} \quad (15)$$
$$\boldsymbol{M}^e = \frac{1}{\rho c_p}\int_{z_i}^{z_j} \boldsymbol{N}^T\boldsymbol{N}dz \quad (16)$$

To solve Eq. (12), an iterative method is needed to calculate the temperature and degree of cure at each time step. Denoting Δt as a time step and t^{n+1} and t^n as the initial and final time instants of the individual step, the temperature and its derivative can be approximated as:

$$\boldsymbol{T}^{n+1} = \boldsymbol{T}^n + \Delta t[\theta\boldsymbol{T}^{n+1} + (1-\theta\boldsymbol{T}^n)] \quad (17)$$
$$\dot{\boldsymbol{T}} = \frac{\boldsymbol{T}^{n+1}-\boldsymbol{T}^n}{\Delta t} \quad (18)$$

The parameter θ can vary between 0 and 1. The value used in this work is $2/3$. The discretized Eq. (12) is expressed as:

$$\left(\frac{\boldsymbol{C}^e}{\Delta t} + \theta\boldsymbol{K}^e\right)\boldsymbol{T}^{n+1} = \left(\frac{\boldsymbol{C}^e}{\Delta t} - \boldsymbol{K}^e(1-\theta)\right)\boldsymbol{T}^n + \boldsymbol{q}^e + \boldsymbol{M}^e\boldsymbol{b}^e \quad (19)$$

The initial value of the degree of cure is zero, and the temperature is equal to room temperature since the part is fully uncured. Thus, it is possible to calculate the two parameters at the next instant from the initial values. The temperature and degree of cure during the cycle can be obtained by proceeding with the iterative method. The temperature and degree of cure are also evaluated, along with the thickness. The two variables are not uniform along the thickness because of the chemical reactions generated during the process and the heating to which the part is subjected. In addition, it is possible to evaluate the behavior of a composite component with different characteristics layer by layer.

2.3 Mechanical properties

The mechanical properties depend greatly on the curing process and particularly on the degree of cure. The instantaneous Young's modulus E_{m} of the resin can be expressed by the following relationship [13]:

$$E_{\mathrm{m}} = (1-\alpha_{mod})\mathrm{E}_{\mathrm{m}}^{\circ} + \alpha_{mod}E_m^{\infty} \quad (20)$$

with:

$$\alpha_{mod} = \frac{\alpha - \alpha_{gel}^{mod}}{\alpha_{diff}^{mod} - \alpha_{gel}^{mod}} \quad (21)$$

The parameters E_m° and E_m^{∞} are the moduli of fully uncured and fully cured resin, α_{gel}^{mod} and α_{diff}^{mod} are the degree of cure at the gelation point and at the end of the cure cycle, respectively. The values considered in this work are $\alpha_{gel}^{mod} = 0.469$ e $\alpha_{diff}^{mod} = 1$. Since the resin is isotropic, the instantaneous shear modulus G_m is calculated as:

$$G_m = \frac{E_m}{2(1+\nu_m)} \quad (22)$$

The Poisson coefficient ν_m is considered constant during the cure cycle.

During the process, a chemical shrinkage is generated due to the exothermic chemical reactions and causes significant deformations in the part. This contribution of volumetric change depends on the increase in the degree of cure through the following relationship [13]:

$$\Delta V_r = \Delta\alpha_{\mathrm{shr}}\, V_{sh}^T = \frac{\alpha}{\alpha_{diff}^{shr}}\, V_{sh}^T \quad (23)$$

where V_{sh}^T is the total shrinkage volume at the end of the resin curing process and $\alpha_{diff}^{shr} = 1$. The shrinkage strain increment is:

Copyright © 2024 by ASME

$$\Delta\epsilon_r = \sqrt[3]{1 + \Delta V_r} - 1 \quad (24)$$

The mechanical properties of the fiber are considered constant and independent of the cure cycle.
The micromechanical model adopted involves using the law of mixtures to find how the mechanical properties of the composite component vary along the thickness during the cure cycle.

3. STRAIN AND STRESS ANALYSIS

The one-dimensional kinematic model adopted in this work is based on CUF [20]. In this work, a Lagrange expansion was used. The displacement field can be written according to CUF through a unified formulation that does not depend on the order of the chosen model:

$$\boldsymbol{u} = \boldsymbol{u}_\tau(y) F_\tau(x,z), \quad \tau = 1, \dots, M \quad (25)$$

where $\boldsymbol{u}_\tau(y)$ is the vector of unknown displacements, $F_\tau(x,z)$ is the expansion function on the cross-section, and M is the number of terms in the expansion. The finite element method allows the approximation of the unknown axial displacements $\boldsymbol{u}_\tau(y)$ to be obtained by introducing the shape functions $N_i(y)$:

$$\boldsymbol{u} = \boldsymbol{u}_{i\tau} N_i(y) F_\tau(x,z), \quad \tau = 1, \dots, M \quad i = 1, \dots, N_N \quad (26)$$

where N_N is the number of nodes in the element and $\boldsymbol{u}_{i\tau}$ are the unknown nodal displacements.

In the analysis of the curing process, the increments of shrinkage and thermal strains at the i-th step are considered as external loads. Using a CHILE approach, a static linear problem can be solved at each time step [19]:

$$\boldsymbol{K}^i \Delta\boldsymbol{u}^i = \Delta\boldsymbol{F}^i \quad (27)$$

where $\boldsymbol{K}^i$ is the i-th stiffness matrix of the model, including the tool, $\Delta\boldsymbol{F}^i$ is the vector of external loads, and $\Delta\boldsymbol{u}^i$ is the unknown displacement increments. Once the solution is found, the stress and strain increments are calculated using the geometric equation and Hooke's law, respectively:

$$\Delta\boldsymbol{\epsilon}^i = \boldsymbol{D}^i \Delta\boldsymbol{u}^i \quad (28)$$

$$\Delta\boldsymbol{\sigma}^i = \boldsymbol{C}^i \Delta\boldsymbol{\epsilon}^i \quad (29)$$

The stiffness matrix $\boldsymbol{K}^i$ consists of several contributions: the stiffness related to the composite part, the stiffness of the shear layer interface model, and finally the stiffness related to the tool. Considering the same subdivision for forces and displacements, the forces applied to the part by the tool can be calculated. The residual deformations and stresses, $\boldsymbol{\epsilon}_r$ and $\boldsymbol{\sigma}_r$, are the sum of the contribution from the curing process ($\Delta\boldsymbol{\epsilon}_c^i$, $\Delta\boldsymbol{\sigma}_c^i$) and that due to tool removal ($\Delta\boldsymbol{\epsilon}_t^i$, $\Delta\boldsymbol{\sigma}_t^i$):

$$\boldsymbol{\epsilon}_r = \sum_{i=1}^{N} \Delta\boldsymbol{\epsilon}_c^i + \Delta\boldsymbol{\epsilon}_t^i \quad (30)$$

$$\boldsymbol{\sigma}_r = \sum_{i=1}^{N} \Delta\boldsymbol{\sigma}_c^i + \Delta\boldsymbol{\sigma}_t^i \quad (31)$$

4. NUMERICAL RESULTS

4.1 Model verification

The verification of the thermochemical model adopted for this work is done by comparison with the solution of a case study presented by Bogetti [22]. The laminate is composed of graphite/epoxy and is 2.54 cm thick. The material characteristics are: $\rho = 1.52 \times 10^3$ kg/m^3, $c_p = 942$ J/(W °C), and $k = 0.4457$ W/(m °C). The curing process involves two holding temperatures at 161 °C and 177°C for 70 min and 127 min, respectively. Fig. 1 shows the comparison of the curing degree and temperature trends predicted by the model used in this work with Bogetti's reference results [22]. The good match of the results demonstrates the good accuracy of the model.

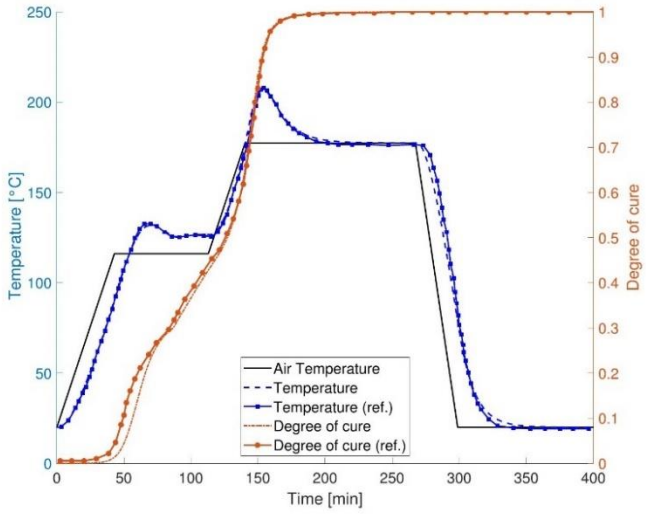

Figure 1: COMPARISON OF TEMPERATURE AND DEGREE OF CURE PREDICTION FOR A GIVEN CURE CYCLE WITH BOGETTI'S REFERENCE RESULTS.

4.2 Layer-wise modeling of a graphite/epoxy composite

This section presents numerical results for a laminate composed of 8552 epoxy resin and unidirectional AS4 carbon fibers. The volume fraction of the fiber is 57.3%. The part analyzed is a flat plate consisting of 8 layers of equal thickness. The stacking sequence considered is $(90/0/90/0)s$. The lamination angle of 90° indicates that the fibers are parallel to the y-axis, while if the angle is 0° the fibers are aligned with the x-axis. Two different laminate thicknesses are considered: in the first case, each layer is 0.2 mm thick; in the second case, the same number of layers was used, but their thickness is 0.4 mm.

Copyright © 2024 by ASME

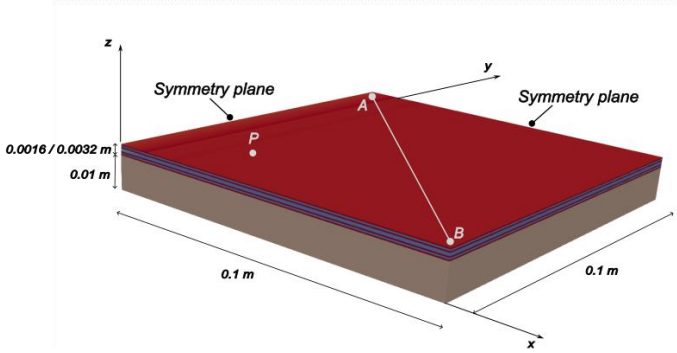

FIGURE 2: MODEL, REFERENCE SYSTEM, AND BOUNDARY CONDITIONS.

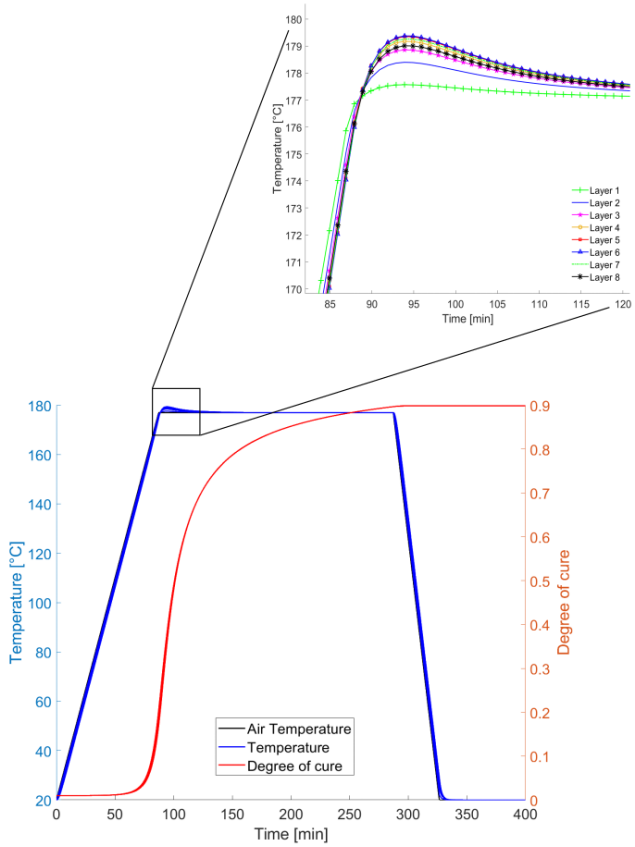

FIGURE 3: CURE DEGREE AND TEMPERATURE FOR EACH LAYER.

The tool material is Invar and has the following characteristics: $E = 150$ GPa, $\nu = 0.28$ and $\beta = 1.56 \cdot 10^{-6}/°C$. The tool's thickness is 10 mm. The geometric model used in this work is shown in Fig. 2.

A simple curing cycle with one hold is considered. It consists of heating to 177 °C at 1.8 °C/min, holding at 177 °C for 200 min, and then cooling the system down. The trends of cure degree and temperature for the eight composite layers during the process are shown in Fig. 3. The numbering of the layers goes from bottom to top.

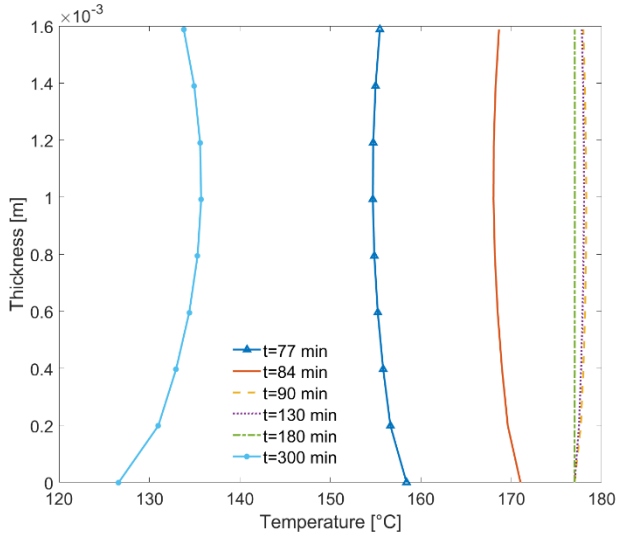

FIGURE 4: TEMPERATURE DISTRIBUTION ALONG THE THICKNESS FOR DIFFERENT TIME INSTANTS OF THE CURE CYCLE RELATED TO THE FIRST CASE.

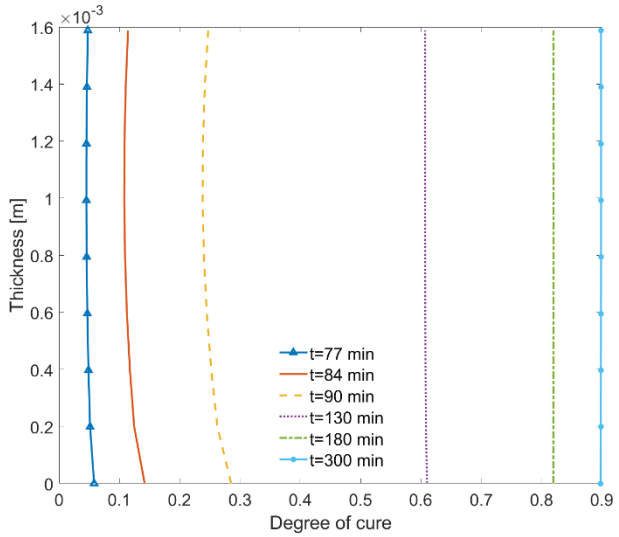

FIGURE 5: DISTRIBUTION OF THE DEGREE OF CURE ALONG THE THICKNESS FOR DIFFERENT TIME INSTANTS OF THE CYCLE OF CARE RELATED TO THE FIRST CASE.

The boundary conditions applied involve convection at the top and an imposed temperature equal to that of the autoclave at the bottom. These conditions greatly influence the temperature of each layer. The temperature evolution through the thickness is analyzed for the first case for different time steps (Fig. 4).
The heat from the autoclave heats the surface layers first, while the middle layers take longer to reach, the temperature profile changes with time steps and the intermediate layers are warmer. This occurs as chemical reactions advance and the internal or exothermic heat generated increases.

Copyright © 2024 by ASME

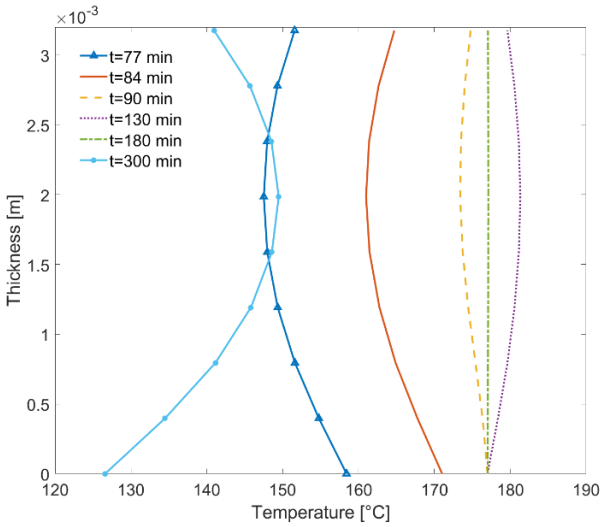

FIGURE 6: TEMPERATURE DISTRIBUTION ALONG THE THICKNESS FOR DIFFERENT TIME INSTANTS OF THE CURE CYCLE RELATED TO THE SECOND CASE.

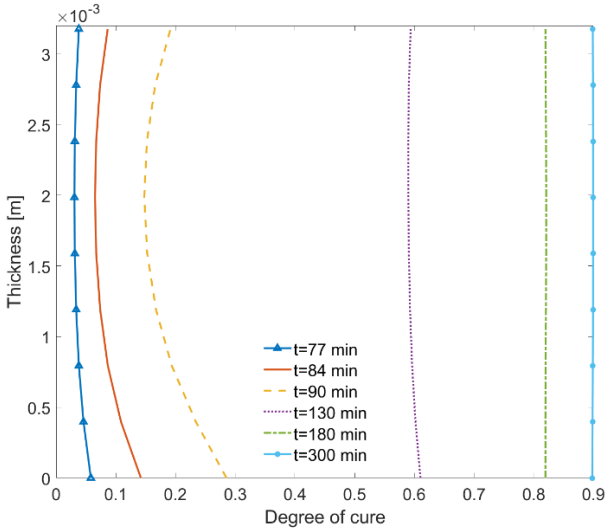

FIGURE 7: DISTRIBUTION OF THE DEGREE OF CURE ALONG THE THICKNESS FOR DIFFERENT INSTANTS OF TIME IN THE CYCLE OF CARE RELATED TO THE SECOND CASE.

The surface layers cool during cooling until the entire part reaches room temperature. The degree of cure is also not uniform along the thickness during the process. It has different profiles depending on the time step considered (Fig. 5). The cure degree at the beginning of the process is higher on the external layers, warmer than in the center. As the process progresses, the degree of cure increases and becomes uniform along the thickness.
To evaluate the influence of thickness, the temperature and cure degree evolutions for the case with double thickness are shown in Fig. 6 and 7. It is evident that the thicker the laminate, the slower the heat transfer from the outer layers to the inner layers. For this reason, the exothermic phase, in which the temperature profile reverses, occurs after a longer time.

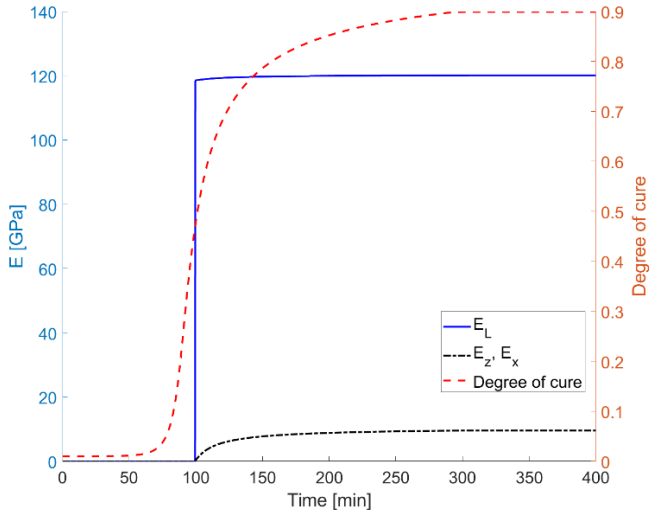

FIGURE 8: AS4/8552 YOUNG MODULI EVOLUTION DURING THE CURING PROCESS FOR THE FIRST CASE.

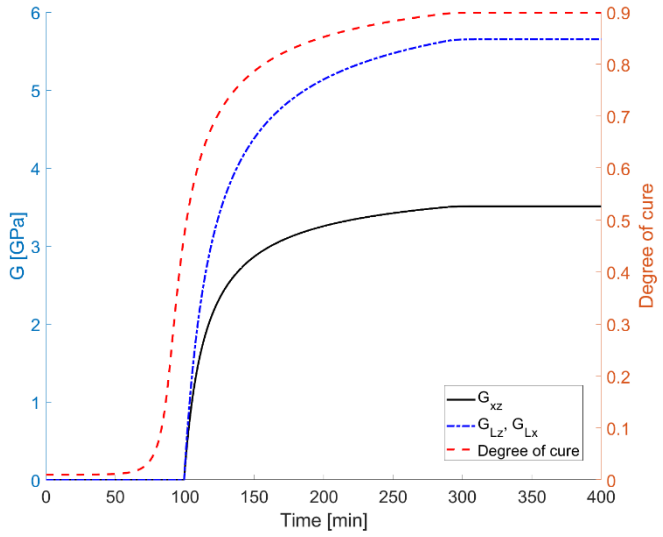

FIGURE 9: AS4/8552 SHEAR MODULI EVOLUTION DURING THE CURING PROCESS FOR THE FIRST CASE.

The mechanical properties of the composite are also highly dependent on the process and particularly on the degree of cure. For this reason, the mechanical properties vary during the process and for each layer. The evolutions over time of Young's moduli and shear moduli related to the fourth layer of the laminate are shown in Figs. 8 and 9. The reported nonzero values of these properties correspond to a degree of cure greater than the gelation point of 0.469.
From the properties evaluated for each layer for the two different thickness cases, it is possible to determine how the part deforms and the distribution of in-plane shear stress.
Only one-quarter of the piece was considered in the analyses. The structure has two planes of symmetry, as shown in Fig. 2.

Copyright © 2024 by ASME

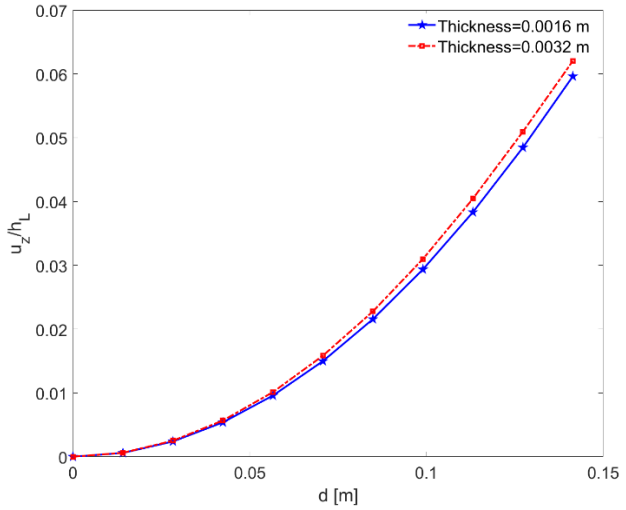

FIGURE 10: DIMENSIONLESS DISPLACEMENTS WITH RESPECT TO INDIVIDUAL LAYER THICKNESS ALONG THE A-B LINE FOR THE TWO DIFFERENT THICKNESS CASES.

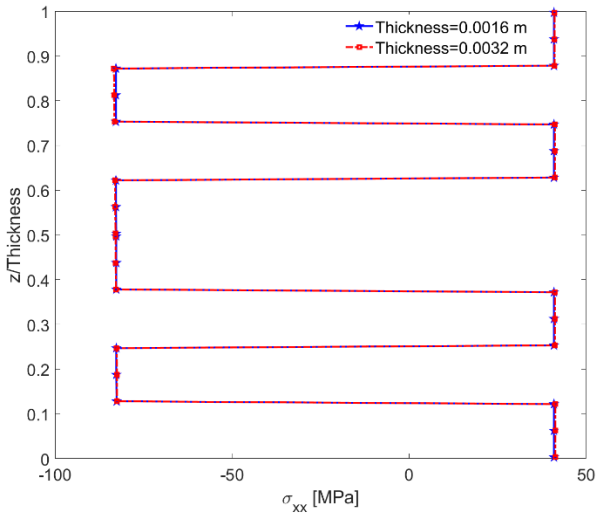

FIGURE 11: THROUGH-THICKNESS DISTRIBUTION OF σ_{xx}.

The model adopted is layer-wise, according to which both material properties and kinematics are described independently layer by layer. Lagrange expansion is used as cross-sectional kinematic approximations. The results obtained, in terms of displacements in z along the d direction joining the two points A and B (Fig. 2), are shown in Fig. 10.

Figure 11, on the other hand, shows the in-plane stress σ_{xx} at point P (Fig. 2), which is located at $x = y = 0.025$ m.

5. CONCLUSION

In this paper, a layer-wise approach allowed temperature and degree of cure to be evaluated independently for each layer. Mechanical properties, dependent on the degree of cure, were exploited to find process-induced displacements and stresses. A refined one-dimensional model based on the Carrera Unified Formulation was applied to a flat plate structure. The results show that the layer-wise approach makes it possible to evaluate how layer-by-layer properties vary during the process. Such variations can affect induced stresses and strains. In future work, more complex geometries and varying material-related parameters could be considered to evaluate their impact on final performance.

ACKNOWLEDGEMENTS

This work was partly supported by the Italian Ministry of Foreign Affairs and International Cooperation, grant number US23GR12.

REFERENCES

[1] M. Hojjati, SV. Hoa. *Some Observations in Curing of Thick Thermosetting Laminated Composites*. Science and Engineering of Composite Materials, vol. 4, no. 2, (1995) 89-108.

[2] G. Fernlund, C. Mobuchon, N. Zobeiry. *2.3 autoclave processing*. Comprehensive Composite Materials II, Elsevier; (2018), 42–62 [chapter 2].

[3] K. D. Potter, M. Campbell, C. Langer, M. R. Wisnom. *The generation of geometrical deformations due to tool/part interaction in the manufacture of composite components.* Composites part A: applied science and manufacturing, 36 (2) (2005) 301-308.

[4] G. Twigg, A. Poursartip, G. Fernlund. *Tool–part interaction in composites processing. Part I: experimental investigation and analytical model*. Composites Part A: Applied Science and Manufacturing, 35(1) (2004) 121-133.

[5] G. Twigg, A. Poursartip, G. Fernlund. *Tool–part interaction in composites processing. Part II: numerical modelling*. Composites Part A: Applied Science and Manufacturing, 35(1) (2004) 135-141.

[6] I. Baran, K. Cinar, N. Ersoy, et al. *A Review on the Mechanical Modeling of Composite Manufacturing Processes*. Arch. Comput. Methods. Eng 24 (2017) 365–395.

[7] C. Albert, G. Fernlund. *Spring-in and warpage of angled composite laminates*. Composites Science and Technology 62(14) (2002) 1895-1912.

[8] H. Hosseini-Toudeshky, B. Mohammadi. *Thermal residual stresses effects on fatigue crack growth of repaired panels bounded with various composite materials*. Composite Structures 89.2 (2009) 216-223.

[9] H. Wang. *Effect of Spring-in Deviation on Fatigue Life of Composite Elevator Assembly*. Applied Composite Materials, 25 (2018) 1357-67.

[10] Y. Yu, I. A. Ashcroft, G. Swallowe. *An experimental investigation of residual stresses in an epoxy–steel laminate*. International Journal of Adhesion and Adhesives, 26, (2006) 511–519.

[11] G. Fernlund, N. Rahman, R. Courdji, M. Bresslauer, A. Poursartip, K. Willden, K. Nelson. *Experimental and numerical study of the effect of cure cycle, tool surface, geometry, and lay-up on the dimensional fidelity of autoclave-processed composite*

Copyright © 2024 by ASME

parts. Composites Part A: Applied Science and Manufacturing, 33 (2002) 341–351.

[12] L. Moretti, P. Olivier, B. Castanié, G. Bernhart. *Experimental study and in-situ FBG monitoring of process-induced strains during autoclave co-curing, co-bonding and secondary bonding of composite laminates* Composites Part A: Applied Science and Manufacturing,142 (2021) 106224.

[13] T.A. Bogetti, Jr J.W. Gillespie. *Process-Induced Stress and Deformation in Thick-Section Thermoset Composite La*minates. Journal of Composite Materials 26(5), (1992).

[14] N. Zobeiry, et al. *Multiscale characterization and representation of composite materials during processing*. Philosophical Transactions of the Royal Society A: Mathematical, Physical and Engineering Sciences 374.2071 (2016): 20150278.

[15] A. Johnston, R. Vaziri, A. Poursartip. *A plane strain model for process-induced deformation of laminated composite structures*. Journal of composite materials, 35(16) (2001) 1435-1469.

[16] Q. Zhu, P. H. Geubelle, M. Li, C. L. Tucker III. *Dimensional accuracy of thermoset composites: simulation of process-induced residual stresses*. Journal of composite materials, 35(24) (2001) 2171-2205.

[17] A. Johnston. *An integrated model of the development of process-induced deformation in autoclave processing of composite structures*. PhD thesis. University of British Columbia, (1997).

[18] P. Hubert. *Aspects of flow and compaction of laminated composite shapes during cure*. Diss. University of British Columbia, (1996).

[19] E. Zappino, N. Zobeiry, M. Petrolo, R. Vaziri, E. Carrera, A. Poursartip. *Analysis of process-induced deformations and residual stresses in curved composite parts considering transverse shear stress and thickness stretching*. Composite Structures, Volume 241, (2020).

[20] E. Carrera, M. Cinefra, M. Petrolo, E. Zappino. *Finite element analysis of structures through unified formulation*. John Wiley & Sons, (2014).

[21] S. Yi, H. H. Hilton, M. F. Ahmad. *A finite element approach for cure simulation of thermosetting matrix composites*. Computers & structures. 64(1-4) (1997) 383-388.

[22] T.A. Bogetti. *Process-induced stress and deformation in thick-section thermosetting composites*. University of Delaware (1989).

Copyright © 2024 by ASME